Evolving Structural Diversity and Metallicity in Compressed Lithium Azide

Dasari L. V. K. Prasad,*,[†] N. W. Ashcroft,[‡] and Roald Hoffmann[†]

[†]Department of Chemistry and Chemical Biology and [‡]Laboratory of Atomic and Solid State Physics, Cornell University, Ithaca, New York 14853, United States

S *Supporting Information*

ABSTRACT: In pursuit of new stable nitrogen-rich phases and of a possible insulator−metal transition, the ground-state electronic structure of lithium azide, LiN_3, is investigated from 1 atm to 300 GPa (∼2-fold compression) using evolutionary crystal structure exploration methods coupled with density functional theoretical calculations. Two new LiN_3 phases, containing slightly reduced and well-separated N_2 units, are found to be enthalpically competitive with the known lithium azide crystal structure at 1 atm. At pressures above 36 GPa nitrogen-rich assemblies begin to evolve. These incorporate NN bond formation beyond that in N_2 or N_3^-. N_6 rings and infinite one-dimensional linear nitrogen chains (structural analogues to polyacetylene) appear. Above 200 GPa quasi-one- and two-dimensional extended puckered hexagonal and decagonal nitrogen layers emerge. The high-pressure phase featuring linear chains may be quenchable to $P = 1$ atm. With increasing pressure the progression in electrical conductivity is from insulator to metal.
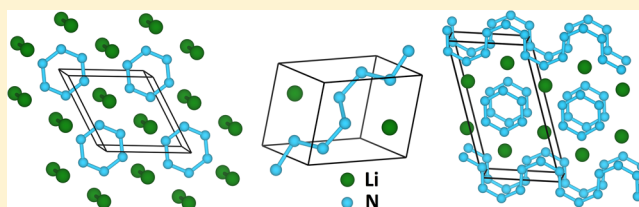
INTRODUCTION

At standard temperature and pressure (STP: $T = 298$ K; $P = 1$ atm), elemental nitrogen is a gas, consisting of molecular diatomic N_2 units. The atoms in the diatomic are bound by stiff covalent triple bonds (N≡N); the molecule's dissociation energy (9.8 eV) is only surpassed by the heteronuclear diatomic CO molecule (11.1 eV).[1] Not many higher molecular or extended structures are known for nitrogen other than N_2, quite a contrast with its neighboring element, carbon. Under normal conditions simple nitrogen catenation (formation of molecules with NN bonds) is limited by the bond strength of the N_2 molecule and substantial barriers (calculated to be >1.8 eV/atom at 1 atm)[2] separating molecular and the less stable at 1 atm oligomeric or polymeric nitrogen allotropes. A few higher elemental molecular units are known, such as N_3,[3] N_4,[4] and the N_5^- anion[5] in the gas phase, and N_5^+ has been isolated in a crystalline phase with AsF_6^- or SbF_6^- counteranions.[6] Tetrahedral N_4 has been a target for synthesis; even though it is ∼182 kcal/mol (∼7.9 eV) less stable than $2N_2$, the barriers to it breaking apart are predicted to be large, ∼60 kcal/mol (∼2.6 eV).[7] The neutrals in this series are all quite unstable, thermodynamically.

Nitrogen does in fact form innumerable stable and metastable chemical compounds, among them some nitrogen-rich ones ($n > 2$, n = number of nitrogen atoms). For instance five- and six-membered heterocyclic ring systems are known with high nitrogen content, up to a maximum of five nitrogen atoms per ring.[8] Recently some adducts of azoles have been synthesized with N_8, N_{10} and N_{11} chain structures.[9−11] To date, N_{11} is the largest known nitrogen-rich chain incorporated in an organic compound, in the chloride salt of 1,1′-(triaz-1-ene-1,3-diyl)bis(1H-tetrazole-5-amine).[11] All nitrogen-rich molecules are energy-rich, in fact potentially explosive, as a consequence of the thermodynamic stability of the product N_2 molecule, and the further gain in entropy in forming small molecules in the gas phase.[8,12]

The application of high pressure to condensed phases opens another route to stabilization of high nitrogen content structures. Theory and experiment have joined to predict and observe a variety of stable or metastable structures for elemental nitrogen and nitrogen-rich phases under compression.[2,13−19] For N_2, the prediction of McMahan et al.[2] that molecular N_2 assumes a monatomic polymeric nitrogen phase (in a three coordinated net called the cubic gauche (cg) phase, cg-N) under pressure, at about 60 GPa, was later confirmed in high-pressure (>110 GPa) and high-temperature (>2000 K) experiments by Eremets et al.[16] The existence of a cg-N phase was also suggested in other high-pressure experiments as well.[17,18] These studies have led in turn to many other theoretical predictions of allotropic forms of nitrogen under pressure.[20−25]

An important class of N-rich systems is that of the azides, containing well-separated molecular-like linear or nearly linear N_3^- complexes ionically or covalently bonded to a variety of stabilizing ions. The first of these to be synthesized were the aryl azides by Griess in 1864 and NaN_3 and HN_3 by Curtius in 1890.[26,27] After the successful synthesis of polymeric cg-N from N_2, many of the alkali-metal azides, AN_3 (A = Li to Cs), were

compressed (LiN_3, 62 GPa at room temperature, RT;[19] NaN_3, 160 GPa at 120−3300 K,[17] 250 GPa at RT−3300 K,[18] 52 GPa at RT;[28] KN_3, 38 GPa at RT;[29] CsN_3, 55 GPa at RT [30]). Perhaps an underlying intuitive hope in these studies was that of reducing the pressures needed to obtain extended nitrogen allotropic structures. Azides already have an "extra" NN bond compared to N_2; this might well be a route to extended nitrogen networks. There seems to be some support for this idea. For instance, in the N_2 and NaN_3 high-pressure experiments of Popov in 2005, cg-N appeared at 50 GPa when one compressed NaN_3 and 127 GPa for the case of pure N_2 (both at RT).[18]

We now report detailed theoretical investigations of the ground-state electronic structure and lattice dynamics of LiN_3 at 1 atm and at high pressures. Surprisingly, we find a welter of new N-rich phases above 36 GPa (~1.3 fold compression). These are structurally unique, featuring cyclic and infinite linear polymer-like nitrogen assemblies, stabilized by Madelung energy involving the lithium ion. The high-pressure nitrogen sublattices we describe are structural analogues of hydrocarbons—benzene and polyacetylene foremost among these. A remarkable feature of all of the high-pressure LiN_3 structures we predict is their metallic nature, even though the manifestation of the charge transfer might classify them as ionic. One of the high-pressure LiN_3 phases which we discuss below ($P6/m$), and its metallic character, has been recently published by Zhang et al.[31]

In search of high-pressure phases for LiN_3, we also stumbled onto two new phases at 1 atm. The remarkable aspect about these two phases is that they return us to well-separated N_2 molecular-like units. The details of the calculations are given at the end of this paper as an Appendix. Every structure calculated in this paper is a ground-state one including zero point energies (ZPE) in the quasiharmonic approximation. (They are incorporated in energetic and enthalpic considerations, unless otherwise noted).

■ RESULTS AND DISCUSSION

LiN_3 Crystal Structure. LiN_3 is an ionic solid ($Li^+N_3^-$) at STP ($T = 298$ K, $P = 1$ atm). It crystallizes in a monoclinic Bravais lattice, space group $C2/m$, with two formula units per cell ($Z = 2$).[32] The LiN_3 structure is isomorphous to the low-temperature (<292 K) phase of NaN_3 (α-NaN_3), so we will refer to the STP-phase α-LiN_3. However, we use a $C2/m$ (I) nomenclature to be consistent with other similar phases (see below) that we predicted at 1 atm. NaN_3 also has a rhombohedral $R\bar{3}m$ phase (β-NaN_3) at high temperature (>292 K).[33] Such a temperature-induced phase transition is not observed in LiN_3 so far.

The LiN_3 $C2/m$ (I) crystal structure consists of Li^+ cations and centrosymmetric linear N_3^- anions packed in a distorted NaCl-type structure, as shown in Figure 1. The cations and anions are arranged alternately in two-dimensional hexagonal close packing (2D hcp) layers. The azide anions are arranged parallel to each other along their molecular axes, these stacked with a tilt angle ($\phi = \theta - 90$) of 11.5° to the 2D hcp layers (see Figure S1 in the Supporting Information (SI) of this paper). The terminating nitrogens of the azide anion are coordinated by three lithium cations; in turn each lithium is coordinated by six nearest end nitrogens of azide anions forming LiN_6 octahedra that are edge-shared, as shown in Figure 1b. The LiN_3 structure can also be viewed as composed of 2D LiN_6 octahedral layers "glued" together with triatomic N_3 needles.
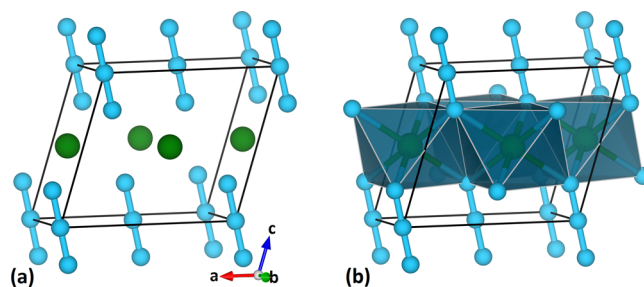
Figure 1. Calculated static ground-state crystal structure of monoclinic LiN_3 $C2/m$ (I) at 1 atm: (a) N_3^- units on the mirror plane of $C2/m$, with central nitrogen occupying the corners of the unit cell; (b) edge-shared LiN_6 octahedra. Li and N are shown in green and blue.

The azide units in LiN_3 are quite well separated (at 1 atm). The experimental N−N separation (1.162 Å)[32] in N_3^- in LiN_3 at 1 atm is similar to that in an isolated N_3^- (1.188 Å), as determined using velocity modulation spectroscopy in the gas phase.[34] The Li−N (2.214 Å) and Li−Li (3.266 Å) separations in LiN_3 are slightly longer than in ionic lithium nitride, Li_3N (Li−N = 1.937 Å)[35] and bcc-Li (Li−Li = 3.02 Å),[36] respectively, at 1 atm. The internuclear separations mentioned above are all experimental; they are in good agreement with our calculated separations (see Table S1 of the SI).

Competing Structures at $P = 1$ atm. The evolutionary crystal structure search prediction schemes that we have used[37] effortlessly found the experimentally known LiN_3 $C2/m$ (I) structure at 1 atm. We also examined for LiN_3 other known EN_3 structure types, E = Na, K, Rb, Co, Cu, Ag, and Hg. The energetics are summarized in Figure S3 of the SI; the result is that the β-NaN_3, HgN_3, and two CuN_3 structure types are within 0.1 eV per formula unit of the α-LiN_3 structure ($C2/m$ (I)). We note that this energy difference is four times smaller than the ZPE (0.4 eV/LiN_3) of α-LiN_3 at 1 atm. All other structure types are higher in energy.

Remarkably, the structure search revealed two nonazide phases that also compete in enthalpy with $C2/m$ (I) at 1 atm. These have the same space group but have $Z = 4$; we refer to them here as $C2/m$ (II) and $C2/m$ (III). The new phases contain N_2 molecular units and Li chains, as shown in Figure 2. $C2/m$ (II) and $C2/m$ (III) are 44 and 153 meV/LiN_3 (ZPEs are included) below the $C2/m$ (I) enthalpy at 1 atm.

The computed bonded NN bond separations in $C2/m$ (II) and $C2/m$ (III) are stretched (1.13−1.16 Å) to a small degree relative to the gas-phase N_2 molecule (1.10 Å). This is consistent with the electronic structures of these phases (to be discussed in detail in subsequent text), which have electrons filling one out of the 12 bands ($Z = 4$) formed from π^* antibonding orbitals of N_2. Because of the low symmetry, and small asymmetric Li−N interactions, not all of the π^* orbitals of all of the N_2 molecules in these phases are equally occupied.

The lithium atoms form quasi-two-dimensional zigzag and linear "element lines" in $C2/m$ (II) and $C2/m$ (III); the Li−Li separations are 2.96 and 2.91 Å, respectively, comparable to the Li−Li separation (3.02 Å) in bcc-Li at 1 atm. Note that there is nothing unusual in this; as cation Li^+ is much smaller than atomic Li. While each N in the N_2 ions is coordinated to two nearest Li atoms in both competing phases, the difference between them lies in the Li−N network. In $C2/m$ (II) each Li is surrounded by six nitrogens, producing LiN_6 octahedra, whereas in $C2/m$ (III) Li has five-coordinated square pyramids (LiN_5), as shown in Figure 2. These polyhedra are edge-shared
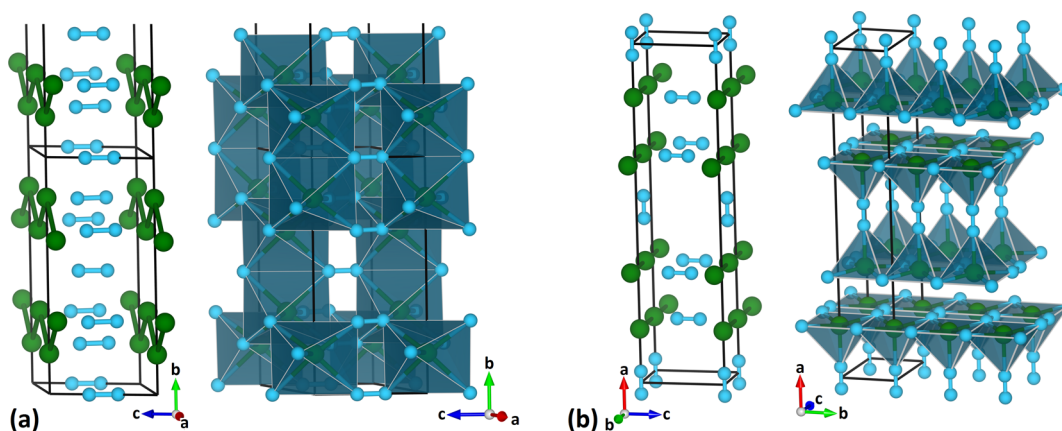
Figure 2. Static ground-state crystal structures of LiN_3 (a) $C2/m$ (II) and (b) $C2/m$ (III) at 1 atm in ball-and-stick and polyhedral representations. The hexagonal holes run along the c-axis in both phases (see text). Octagonal holes can be seen in $C2/m$ (III) along the b-axis. Blue = N; green = Li.

in 2D Li−N layers, and these layers are connected by N_2 units in a way that leaves hexagonal and octagonal holes in the Li−N layers. No such holes exist in $C2/m$ (I) (see Figure S4 of the SI for layer and polyhedral edge-sharing representations of LiN_3 phases).

The first thought on finding a structure featuring N_2 molecules (albeit that they are slightly reduced) and Li chains is that the ionic LiN_3 is trying to dissociate to N_2(s) and Li(s). Is there a driving mechanism for such a reaction? The calculated heat of formation (ΔH_f) of the lithium azide $C2/m$ (I) phase in the ground state is −0.55 eV/LiN_3; the experimental heat of formation at 298 K (ΔH°_f) is +0.11 eV/LiN_3.[38,39] The difference is higher than expected, but (a) the experimental figure is somewhat uncertain and (b) the calculation gives a ground-state (T → 0) value; the experimental value is for 298 K. The calculated negative heat of formation of the azide would seem to argue against the existence of stable alternative structures that contain N_2 molecules (partially reduced). But there could well be some gain in stabilization from Madelung energies in such structures, so we cannot reject them as unreasonable. An alternative decomposition of the azide, $3LiN_3 \rightarrow Li_3N + 4N_2$, is just about thermoneutral. However, we found no structures that incorporate elements of the ionic nitride with N_2 molecules.

A reviewer has suggested that our density functional theory (DFT) calculations might be misleading here, in indicating stability for the "molecular" complexes. A recalculation of the $C2/m$ (I) and (III) structures with the HSE06 functional found the N_2-containing structure (III) 0.10 eV per LiN_3 above (I), which still leaves it competitive. We might add that our confidence in the structural search was reinforced by computations (to be reported elsewhere) on Li_2N_2, which found the observed structure.[40]

Higher Pressure Phases: N_6 Rings. The structures we have described in the preceding text all quickly destabilize as the pressure rises, with the exception of the known $C2/m$ (I) structure, which persists at least up to 36 GPa. A number of interesting, novel structures emerge above that pressure, where the nitrogen sublattices resemble well-known hydrocarbons— benzene and polyacetylene. The computed enthalpies of the various stable and metastable phases as a function of pressure are shown in Figure 3 (see Figures S5−S7 of the SI for a complete list of phases found in our calculations).

The first stable high-pressure phase beyond $C2/m$ (I) appears at 36 GPa and remains stable at higher pressures, up to
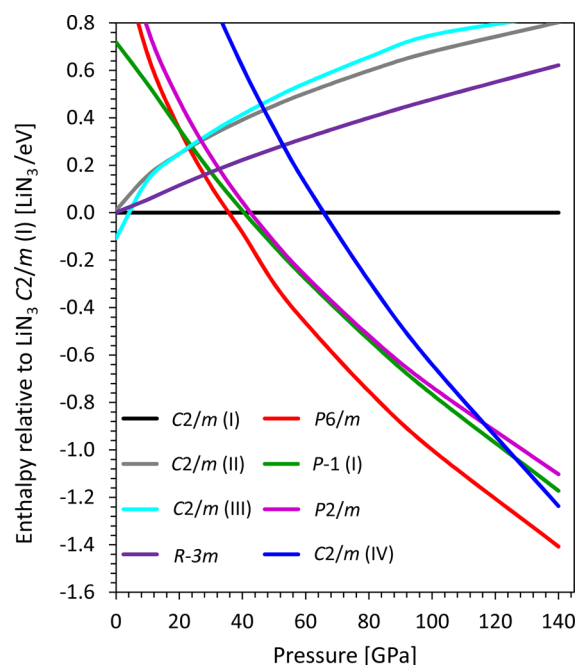
Figure 3. Static ground-state enthalpies (per LiN_3) of various LiN_3 structures relative to the experimental α-LiN_3 $C2/m$ (I) phase. Zero point energies are not included.

190 GPa (see Figure 3). In this hexagonal $P6/m$ structure (Figure 4), the nitrogen sublattice adopts benzene-like planar six-membered N_6 rings. The rings form columnar hcp arrays embedded in lithium hcp element lines, as shown in Figure 4a.

The N_6 rings are perfectly hexagonal, D_{6h}. However, as the $P6/m$ space group indicates, the N_6 ring mirror planes and the $P6/mmm$ Li sublattice are not in registry—if they were, LiN_3 would be in the $P6/mmm$ space group. At the onset of its region of stability at 36 GPa, $P6/m$ LiN_3 is characterized by rotational disorder in the N_6 rings, with imaginary frequencies as a consequence. But, above 40 GPa the phonon calculations suggest that the $P6/m$ phase is then dynamically stable.

The Li−Li separation in the Li element lines (2.34 Å, 60 GPa) is 0.1 Å longer than in fcc-Li at 60 GPa, and the Li−N separation (1.92 Å) is in line with the LiN separation in ionic solid γ-Li_3N (1.90 Å) at the aforementioned pressure. Each N of an N_6 ring is coordinated by two nearest Li atoms that are above and below the nitrogen ring plane, and each Li is six-
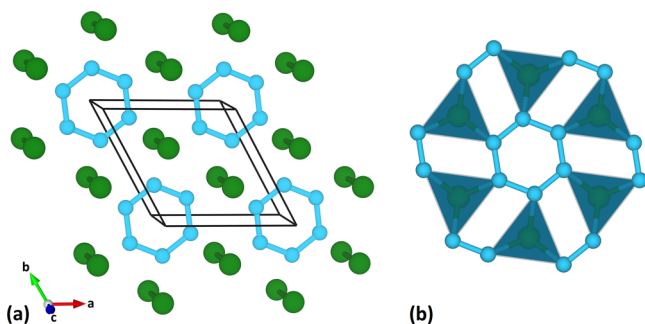
Figure 4. (a) Static ground-state crystal structure of LiN_3 $P6/m$ at 60 GPa. (b) Li−N network around the N_6 ring shown in polyhedral representation. Blue = N; green = Li.

coordinated by nearby N atoms, forming triangular prisms whose triangular bases are face-shared along the c-axis (see Figure 4b).

All six NN bonds in the N_6 units in LiN_3 are identical, 1.31 Å at 60 GPa, which is shorter than the NN bond (1.36 Å) in cg-N at the same pressure (see Figure S2 of the SI for evolution of NN separations under pressure). Another comparison might be with an isolated N_6^{2-} molecular ring, optimized at 1 atm; this has the same NN separation. The shortest inter-ring NN separation in the $P6/m$ is 2.59 Å, and the separation from an N_6 ring nitrogen to one above it along the c-axis is 2.34 Å (at 60 GPa). The inference is that the N_6 rings in LiN_3 are quite well separated.

The nitrogen hexagons in the N_6^{2-} sublattice of LiN_3 are planar. An isolated planar N_6^{2-} ring (which is expected to be subjected to a Jahn−Teller distortion) deforms to a C_{2v} "boat" form (see Figure S8 in SI for C_{2v} N_6^{2-}). Starting the optimization in the LiN_3 crystal structure with such a boat ring returns the structure to the $P6/m$ phase with a planar N_6 ring upon optimization. This points to the importance of Li−N Madelung energy in stabilizing the planar N_6 rings in LiN_3, and the whole LiN_3 crystal structure.

It may be relevant here to mention the long story of discrete molecular N_6. The replacement of CH in benzene by N is a formally "isoelectronic" one. And indeed $(CH)_{6-n}N_n$ rings are known molecules for n = 1 −4. But, cyclic N_6 is not known experimentally. The molecule has attracted great theoretical interest. It is clearly not very stable, but could it be a local minimum? The theoretical discussion has gone back and forth on this;[41] the latest evidence is that there is no barrier for this ring to spontaneously decompose into three N_2 molecules.

As we were completing this work, a study of LiN_3 under pressure appeared by Zhang et al.[31] It reported and analyzed the same $P6/m$ structure we discuss here.

Given that we found benzenoid structures albeit that they are negatively charged (N_6^{2-}), we also looked for structures that incorporate N_4^{2-} units, isoelectronic with the aromatic cyclobutadiene dianion ring. The isolated molecular dianion, capped by two lithium counterions, appears to be metastable.[42] But, all of the structures we calculated for LiN_3 that incorporate such four-membered rings emerged as substantially less stable than the structures discussed so far.

High-Pressure Phases: Chains. In the stability range of $P6/m$ (36−190 GPa, or 1.3- to 1.9-fold compression) some other low-symmetry phases appear as metastable, with intriguing structures. The nitrogen sublattice in one of these, $P\bar{1}$ (I), takes on a polyacetylene-like infinite linear chain structure. In another, $P2/m$, the unit cell is composed of N_6

rings and wavelike nitrogen assemblies, as shown in Figure 5a,b. The linear and wavelike N-chains in $P\bar{1}$ (I) and $P2/m$ have the
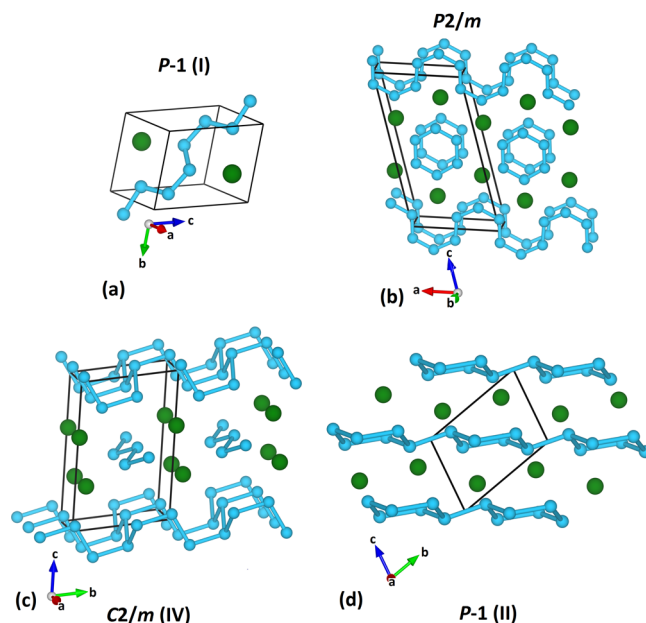
Figure 5. Static ground-state crystal structures of LiN_3: (a) $P\bar{1}$ (I), (b) $P2/m$, (c) $C2/m$ (IV), and (d) $P\bar{1}$ (II) at 60, 100, 200, and 200 GPa, respectively. All of the structures shown here are metallic.

closest NN separations that are in the range of 1.32−1.29 Å at 60 GPa. The N_6 rings and lithium sublattice in $P2/m$ are similar to those in the $P6/m$ phase. We note that these phases in our calculations are only metastable. That such structures should arise is entirely plausible, following the electronic analogy of CH and N. It takes ~200 GPa (1.9 fold compression) in our calculations for LiN_3 to spawn extended nitrogen nets.

Above 190 GPa and in the ground state two new phases are at lower enthalpy than $P6/m$. They are $C2/m$ (IV) and $P\bar{1}$ (II). These high-pressure phases have puckered extended 2D decagonal and quasi-2D hexagonal nitrogen layers, as shown in Figure 5c,d. These nitrogen nets are structurally somewhat similar to black phosphorus (A17) and arsenic (A7) structures, respectively.[43] The A17 and A7 networks contain puckered six-membered rings. Six out of 10 nitrogens in the puckered decagons of $C2/m$ (IV), and two out of six in $P\bar{1}$ (II) hexagons are three-coordinated within the nitrogen network. The NN separations (1.30−1.33 Å, 200 GPa) in these nets are similar to the known three-coordinated cg-N NN separations (1.31 Å, 200 GPa). $C2/m$ (IV) also contains infinite zigzag nitrogen chains. The quasi-2D and 1D nitrogen frameworks in these structures are separated by a lithium sublattice (Figure 5c). The structure $C2/m$ (IV) remains as the most stable phase of LiN_3 until 500 GPa, as shown in enthalpic comparison of Figure 6. The phonons were calculated for all of the structures we investigated (see SI, Figure S9). In fact all of the structures we calculated exhibit no imaginary frequencies in their pressure ranges and are thus vibrationally stable.

We did not find any 3D nitrogen nets in our structure search, at least in the pressure range studied (1 atm to 500 GPa). A model LiN_3 superlattice (Li_8N_{24}) containing a 3D nitrogen net was constructed by filling some (there are several possibilities; the lowest enthalpy structure is reported here) of the holes in cg-N. Optimization of a Li_8N_{24} model built this way leads to a
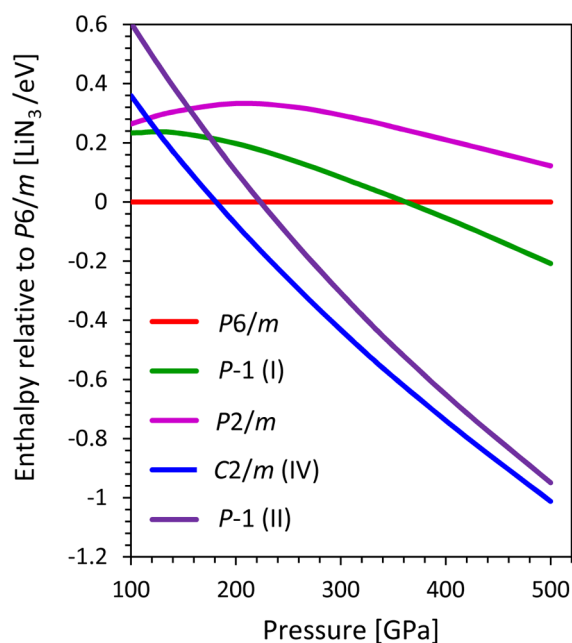
Figure 6. Static ground-state enthalpies of various LiN$_3$ structures relative to the P6/m phase. Zero point energies are not included.

Figure 7. Calculated Perdew−Burke−Enzerof (PBE) electronic band structure and total density of states (per-electron) of static LiN$_3$ phases at 1 atm: (top) C2/m (I) (Z = 2); (bottom) C2/m (III) (Z = 4). The dashed lines mark the energy of the highest occupied crystal orbital. Schematic molecular orbital energy level diagrams of N$_3^-$ and N$_2$ molecules are shown beside the corresponding C2/m (I) and C2/m (III) densities of states, respectively.

structure with N$_2$ units and infinite nitrogen chains. This structure is 0.9 eV/LiN$_3$ higher in enthalpy than LiN$_3$ P6/m at 60 GPa. The computed structure of Li$_8$N$_{24}$ is given in SI (Figure S10).

Quenchable High-Pressure LiN$_3$ Phases? The nitrogen sublattice in LiN$_3$ evolved from molecular N$_2$ → N$_3$ → N$_6$ → extended 1D and 2D nitrogen nets under pressure. We next inquire about the possibilities that any of these nets return to 1 atm, while retaining their structures. Among all of the phases studied here $P\bar{1}$ (I) is the only one that has no imaginary phonons from its range of stability down to P = 1 atm. However, at 1 atm, it is 0.7 eV/LiN$_3$ in enthalpy above the C2/m (I) phase. If the barrier to isomerization to LiN$_3$ (or decomposition to elements) can protect $P\bar{1}$(I), then perhaps it could be detected. Other stable and metastable phases identified at high pressures (>36 GPa) have imaginary phonons when the pressure is lowered (<10 GPa).

Metal to Insulator, and Then Back to Metal Transitions. The calculated electronic band structure and total density of states of LiN$_3$ C2/m (I) and C2/m (III) phases at 1 atm are shown in Figure 7. The electronic structures of alternative (at low pressure) $R\bar{3}m$ and C2/m (II) phases are similar to C2/m (I) and C2/m (III), respectively; the details are reported in the SI, Figure S11. The crystal orbitals—the bands in C2/m (I) and C2/m (III)—are grouped, with significant gaps separating them; the implication is that they are derived from quite localized molecular orbitals of N$_3^-$ and N$_2$ molecules (shown in Figure 7). In both of these solids the valence bands and lowest unoccupied portion of the conduction bands belong to nitrogen; lithium bands are located 6 eV above the Fermi level (E$_F$) and higher. The implication is of predominantly ionic Li−N interactions.

Low-pressure C2/m (I) LiN$_3$ [Li$^+$N$_3^-$] should be an insulator, as one would expect from the molecular orbital (MO) diagram of the azide anion (Figure 7, top right). The calculated Perdew−Burke−Enzerof (PBE) band gap is 3.2 eV (using HSE06 it is 5.1 eV); a direct gap occurs at Z-point in the first Brillouin zone. No experimental band gap data are available

for comparison. Calculated band gaps for C2/m (I) in other theoretical studies are comparable, within the errors of the DFT methodology.[44,45]

The competing C2/m (III) phase, the one with N$_2$, units also has a direct band gap (at the C-point in the zone) of 4.6 eV. However, this phase, [Li$_4^{4+}$(6N$_2$)$^{4-}$] is at first sight metallic, as a consequence of transfer of the lithium electrons to the π^* antibonding orbitals of the N$_2$ conduction band (Figure 7, bottom).

Is C2/m (III) metallic or on the verge of being a Mott insulator? A spin-polarized calculation did not split the partially filled π^* band. Introduction of a Hubbard U (the onsite Coulomb repulsion) using Dudarev's approach[46] has no effect on the band structure, until the U$_{eff}$ value is as large as 10 eV. At U$_{eff}$ = 10 eV, C2/m (III) becomes half-metallic (μ_B = 1.04 per 2 N$_2$ molecules at 1 atm), as shown in Figure 8. We think that such a large U$_{eff}$ is unrealistic,[47] and believe the C2/m (III) (and its related C2/m (II) structure) will indeed be metallic.

The P6/m structure, the one containing benzenoid rings, is metallic throughout the pressure range investigated here (1 atm to 500 GPa, (~2.6-fold compression). The calculated band structure at 60 GPa is shown in Figure 9a,b. Note the molecular-like well-separated lower bands. Akin to C2/m (III), lithium transfers its valence 2s electron to the π^* antibonding orbitals of the N$_6$ benzene-like ring. The bands between +4 and −14 eV are predominantly nitrogen 2p states, with some N 2s mixing, while the bands below −14 eV are N 2s states. The top valence bands and the conduction bands near the Fermi level are analogous to the well-known benzene π orbitals (see SI Figure S12). The high-pressure $P\bar{1}$ (1) and C2/m (IV) phases (with chains and extended layers) are broadly similar in their electronic structure to P6/m. These phases are calculated to be
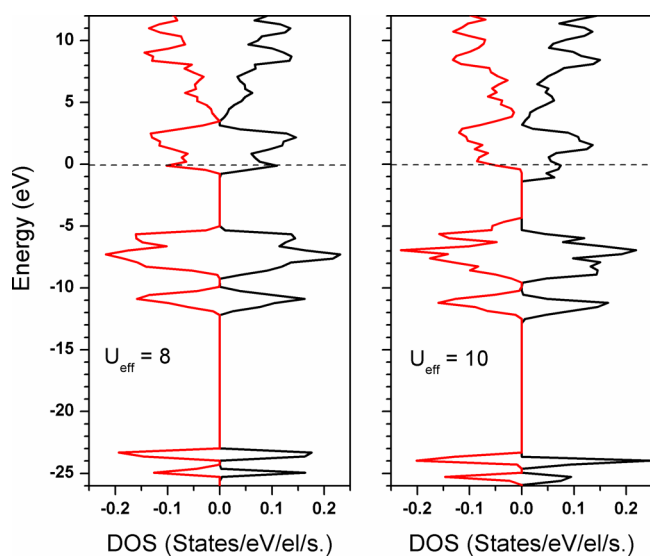
Figure 8. GGA + *U* total spin polarized density of states of *C2/m* (III) at U_{eff} = 8 and 10 eV. The structure is nonmagnetic for U_{eff} below 8 eV; above it, half-metallic.

metallic; the bands crossing the Fermi level are π-like with some lone-pair character. The densities of states (per-electron) are shown in Figure 9c,d at 100 and 200 GPa, respectively. In $P\bar{1}$ (1) an interesting gap opens at an equivalent of four electrons above the Fermi level (as integrated on the DOS plot). The band structures and band projected charge density plots near the Fermi level are shown in the SI, Figure S12.

The findings of metallicity or lack of it were checked by calculations with an HSE06 hybrid functional. They remain as reported in preceding text.

In the sequence of LiN₃ structural phase transitions was found to be as follows: *C2/m* (III) [1 atm] → *C2/m* (I) [3 GPa] → *P6/m* [36 GPa] → *C2/m* (IV) [190 GPa]; the predicted electrical properties thus change from metal → insulator → metal with increasing pressure. This is an unusual reentrant sequence but also seen for a metal–electride–metal

sequence for Li itself and also for Na under pressure.[48] In LiN₃ we looked for an electride phase but did not find one. But, here our structures are not accompanied by an electride phase. The presumption in this unusual progression in electronic behavior is that the N₂-containing low-pressure phases are real, as computed. If one goes directly from the low-pressure *C2/m* (I) structure to the high-pressure phases, the progression is more typical, namely, insulator to metal.

While there is no evidence to date for structural or electrical phase transitions in high-pressure LiN₃, in experiments carried out up to 60 GPa,[19] for NaN₃ there is strong evidence for both in terms of structural phase transitions (>19 GPa) and an observed darkening of the sample above 50 GPa.[17]

■ CONCLUSION

Structural explorations of lithium azide from 1 atm to 500 GPa (~2.6-fold compression) have been investigated within density functional theory. In addition to the experimentally known monoclinic LiN₃ (*C2/m* (I)) phase, two other competing phases containing N₂ units that are slightly reduced are predicted at 1 atm. Interestingly these phases are metallic but become unstable above 3 GPa, corresponding to quite small compressions. At pressures above 36 GPa, N₆ rings and infinite-linear and wave-like nitrogen-rich assemblies in LiN₃ structures then emerge as the most stable phases.

A notable feature of all of the high-pressure phases is that they are also metallic. Given that the constituents are light elements, the phonon energy scales are quite high (see above), so the prospect of superconductivity may therefore be worth pursuing. The N₆ and infinite N-chain sublattices in *P6/m* and $P\bar{1}$ (I) phases can be structurally regarded as hydrocarbon analogues of benzene and polyacetylene, except that they emerge as negatively charged. At very high pressures (>200 GPa) quasi-one- and two-dimensional extended puckered hexagonal and decagonal nitrogen layers are the stable arrangements. The calculated ground-state thermochemistry and density functional perturbation theory–phonon calculations indicate that these phases are enthalpically and dynamically stable.
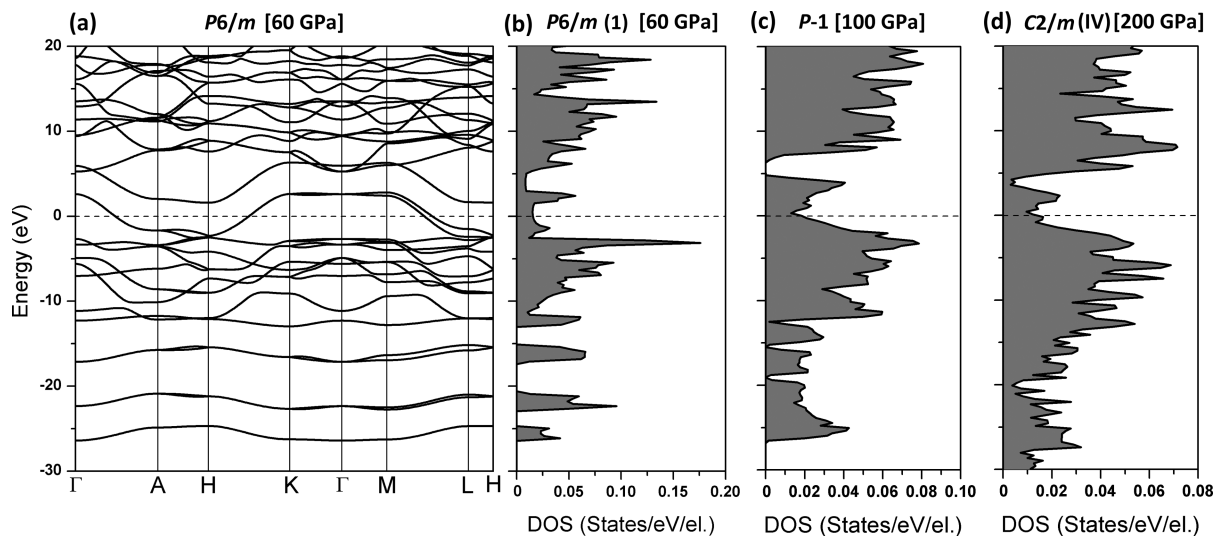
Figure 9. (a, b) Calculated PBE electronic (and metallic) band structure and total density of states (per-electron) of static LiN₃ *P6/m* at 60 GPa, (c) DOS of $P\bar{1}$ (1) at 100 GPa, and (d) DOS of *C2/m* (IV) at 200 GPa. The Fermi energy (E_F) level is set to zero. See the SI for the band structures of $P\bar{1}$ (1) and *C2/m* (IV).

The $P\bar{1}$ (I) phase may be quenchable if kinetically persistent. The N_6 and infinite N-chain containing stable and metastable $P6/m$ and $P\bar{1}$ (I) phases dominating in the high-pressure landscape (up to 200 GPa) are fascinating, and provide in our view an impetus to reinvestigate LiN_3 in the high-pressure regime, to seek these nitrogen-rich assemblies.

■ APPENDIX

Theoretical Methodology

Lithium azide crystal structures were explored using evolutionary structure search algorithms as implemented in the XtalOpt program.[37] The structures were optimized using density functional theory (DFT), as implemented in the Vienna ab initio Simulation Package (VASP).[49] The generalized gradient approximation of Perdew–Burke–Enzerof[50] as the energy functional, and the Projector Augmented Wave (PAW) method for the electron-ion interaction was used.[51,52] The PAW potentials represent the valence electrons of Li ($1s^2, 2s^1$), N ($2s^2, 2p^3$) with cut-off radii 1.7 and 1.5 a_0 (a_0 being the Bohr radius) respectively. A plane-wave basis set cutoff of 650 eV, self-consistent field tolerance of 0.1×10^{-6} eV/atom, zone sampling on a grid of spacing $2\pi \times 0.01$ Å^{-1}, and 10^{-3} eV/Å threshold of forces ("force" in a classical sense) on atoms guaranteed good convergence. HSE06 calculations[53,54] were done by setting the range-separation parameter 0.2 as implemented in VASP. The molecular calculations were carried out at PBEPBE/6-31+g(d,p) level of theory using Gaussian 09 program.[55]

The XtalOpt structure searches were carried out for LiN_3 considering $Z = 1, 2$, and 4, and pressures $P = 1$ atm, 10, 50, 100, 200, and 300 GPa. We have followed a structure search approach similar to the one we used in our $LiNH_2$ study.[56] Phonon calculations were carried out for the low enthalpy phases using the PHONOPY code[57] which is interfaced with VASP gamma point phonon calculations, at the density functional perturbation theory (DFPT) level.[58] The space groups of the crystal structures were identified using FINDSYM[59] and Spglib[60] programs. The XRD patterns of LiN_3 phases were calculated using the Reflex module in Materials Studio.[61] The crystal structure graphics were produced using VESTA.[62]

■ ASSOCIATED CONTENT

Ⓢ Supporting Information

Crystal structures of lithium azide with tilt angle indicated, internuclear separations in LiN_3 phases, energetics of various LiN_3 structures (at 1 atm) in the known EN_3 structure types, layer and polyhedral representations of LiN_3 phases at 1 atm, pressure vs enthalpy plots of all of the interesting ground-state LiN_3 structures obtained in the structure search, structure of the N_6^{2-} molecule, phonon density of states of the most stable LiN_3 phases, optimized crystal structure of Li_8N_{24}, electronic band structure and density of states of LiN_3 phases from 1 atm to high pressures, band projected charge density isosurface plots of high-pressure LiN_3 phases, optimized crystallographic information of various LiN_3 crystal structures, and calculated XRD patterns of LiN_3 phases. This material is available free of charge via the Internet at http://pubs.acs.org.

■ AUTHOR INFORMATION

Corresponding Author

*E-mail: pld48@cornell.edu.

Notes

The authors declare no competing financial interest.

■ REFERENCES

(1) Darwent, B. B. Bond Dissociation Energies in Simple Molecules. *Natl. Stand. Ref. Data Ser. (U. S., Natl. Bur. Stand.)* **1970**, *52*, 23−39.

(2) Mailhiot, C.; Yang, L. H.; McMahan, A. K. Polymeric Nitrogen. *Phys. Rev. B: Condens. Matter Mater. Phys.* **1992**, *46*, 14419−14435.

(3) (a) Hansen, N.; Wodtke, A. M. Velocity Map Ion Imaging of Chlorine Azide Photolysis: Evidence for Photolytic Production of Cyclic-N_3. A. *J. Phys. Chem.* **2003**, *107*, 10608−10614. (b) Larson, C.; Yuanyuan, Samartzis, P. C.; Quinto-Hernandez, A.; Lin, J. J.-M.; Ching, T. T.; Chaudhuri, C.; Lee, S. H.; Wodtke, A. M. Observation of Photochemical C−N Bond Cleavage in CH_3N_3: A New Photochemical Route to Cyclic N_3. *J. Phys. Chem. A* **2008**, *112*, 1105−1111.

(4) Cacase, F.; de Petris, G.; Troiani, A. Experimental Detection of Tetranitrogen. *Science* **2002**, *295*, 480−481.

(5) Vij, A.; Pavlovich, J. G.; Wilson, W. W.; Vij, V.; Christe, K. O. Experimental Detection of the Pentaazacyclopentadienide (Pentazolate) Anion, cyclo-N_5^-. *Angew. Chem., Int. Ed.* **2002**, *41*, 3051−3054.

(6) (a) Christe, K. O.; Wilson, W. W.; Sheehy, J. A.; Boatz, J. A. N_5^+: A Novel Homoleptic Polynitrogen Ion as a High Energy Density Material. *Angew. Chem., Int. Ed.* **1999**, *38*, 2004−2009. (b) Vij, A.; Wilson, W. W.; Vij, V.; Tham, F. S.; Sheehy, J. A.; Christe, K. O. Polynitrogen Chemistry. Synthesis, Characterization, and Crystal Structure of Surprisingly Stable Fluoroantimonate Salts of N_5^+. *J. Am. Chem. Soc.* **2001**, *123*, 6308−6313.

(7) Brincka, T.; Bittererova, M.; Östmark, H. Electronic Structure Calculations as a Tool in the Quest for Experimental Verification of N_4. *Theor. Comput. Chem.* **2003**, *12*, 421−439.

(8) Gao, H.; Shreeve, J. M. Azole-Based Energetic Salts. *Chem. Rev.* **2011**, *111*, 7377−7436.

(9) Li, Y. C.; Qi, C.; Li, S. H.; Zhang, H. J.; Sun, C. H.; Yu, Y. Z.; Pang, S. P. 1,1′-Azobis-1,2,3-triazole: A High-Nitrogen Compound with Stable N_8 Structure and Photochromism. *J. Am. Chem. Soc.* **2010**, *132*, 12172−12173.

(10) (a) Klapötke, T. M.; Piercey, D. G. 1,1′-Azobis(tetrazole): A Highly Energetic Nitrogen-Rich Compound with a N_{10} Chain. *Inorg. Chem.* **2011**, *50*, 2732−2734. (b) Klapötke, T. M.; Piercey, D. G.; Stierstorfer, J. Amination of Energetic Anions: High-Performing Energetic Materials. *Dalton Trans.* **2012**, *41*, 9451−9459. (c) Tang, Y.; Yang, H.; Shen, J.; Wu, B.; Ju, X.; Lu, C.; Cheng, G. Synthesis and Characterization of 1,1′-Azobis(5-methyltetrazole). *New J. Chem.* **2012**, *36*, 2447−2450.

(11) (a) Tang, Y.; Yang, H.; Wu, B.; Ju, X.; Lu, C.; Cheng, G. Synthesis and Characterization of a Stable, Catenated N11 Energetic Salt. *Angew. Chem., Int. Ed.* **2013**, *52*, 4875−4875. (b) Zhang, Q.; Shreeve, J. M. Growing Catenated Nitrogen Atom Chains. *Angew. Chem., Int. Ed.* **2013**, *52*, 8792−8794.

(12) Fair, H. D.; Walker, R. F. *Energetic Materials*, Vol. *1*; Plenum: New York, 1977.

(13) Eremets, M. I.; Hemley, R. J.; Mao, H. K.; Gregoryanz, E. Semiconducting Non-Molecular Nitrogen up to 240 GPa and its Low-Pressure Stability. *Nature* **2001**, *411*, 170−174.

(14) Goncharov, A. F.; Gregoryanz, E.; Mao, H. K.; Liu, Z.; Hemley, R. J. Optical Evidence for a Nonmolecular Phase of Nitrogen above 150 GPa. *Phys. Rev. Lett.* **2000**, *85*, 1262−1265.

(15) Gregoryanz, E.; Goncharov, A. F.; Hemley, R. J.; Mao, H. K. High-Pressure Amorphous Nitrogen. *Phys. Rev. B: Condens. Matter Mater. Phys.* **2011**, *64*, No. 052103.

(16) Eremets, M. I.; Gavriliuk, A. G.; Trojan, I. A.; Dzivenko, D. A.; Boehler, R. Single-Bonded Cubic form of Nitrogen. *Nat. Mater.* **2004**, *3*, 558−563.

(17) Eremets, M. I.; Popov, M.; Trojan, I. A.; Denisov, V. N.; Boehler, R.; Hemley, R. J. Polymerization of Nitrogen in Sodium Azide. *J. Chem. Phys.* **2004**, *120*, 10618−10623.

(18) Popov, M. Raman and IR Study of High-Pressure Atomic Phase of Nitrogen. *Phys. Lett. A* **2005**, *334*, 317−325.

(19) Medvedev, S. A.; Trojan, I. A.; Eremets, M. I.; Palasyuk, T.; Klapötke, T. M.; Evers, J. Phase Stability of Lithium Azide at Pressures up to 60 GPa. *J. Phys.: Condens. Matter* **2009**, *21*, No. 195404.

(20) Mattson, W. D.; Sanchez-Portal, D.; Chiesa, S.; Martin, R. M. Prediction of New Phases of Nitrogen at High Pressure from First-Principles Simulations. *Phys. Rev. Lett.* **2004**, *93*, No. 125501.

(21) Zahariev, F.; Hooper, J.; Alavi, S.; Zhang, F.; Woo, T. K. Low-Pressure Metastable Phase of Single-Bonded Polymeric Nitrogen from a Helical Structure Motif and First-Principles Calculations. *Phys. Rev. B: Condens. Matter Mater. Phys.* **2007**, *75*, No. 140101.

(22) Alemany, M. M. G.; Martins, J. L. Density-Functional Study of Nonmolecular Phases of Nitrogen: Metastable Phase at low Pressure. *Phys. Rev. B Condens. Matter Mater. Phys.* **2003**, *68*, No. 024110.

(23) Ma, Y.; Oganov, A. R.; Li, Z.; Xie, Y.; Kotakoski, J. Novel High Pressure Structures of Polymeric Nitrogen. *Phys. Rev. Lett.* **2009**, *102*, No. 065501.

(24) Pickard, C. J.; Needs, R. J. High-Pressure Phases of Nitrogen. *Phys. Rev. Lett.* **2009**, *102*, No. 125702.

(25) Wang, X.; Wang, Y.; Miao, M.; Zhong, X.; Lv, J.; Cui, T.; Li, J.; Chen, L.; Pickard, C. J.; Ma, Y. Cagelike Diamondoid Nitrogen at High Pressures. *Phys. Rev. Lett.* **2012**, *109*, No. 175502.

(26) Griess, P. On a New Class of Compounds in Which Nitrogen Is Substituted for Hydrogen. *Proc. R. Soc. London* **1864**, *13*, 375−384.

(27) Curtius, T. Ueber Stickstoffwesserstoffsaure (Azomid) N₃H. *Berichte* **1890**, *23*, 3023−3033.

(28) Zhu, H.; Zhang, F.; Ji, C.; Hou, D.; Wu, J.; Hannon, T.; Ma, Y. Pressure-Induced Series of Phase Transitions in Sodium Azide. *J. Appl. Phys.* **2013**, *113*, No. 033511.

(29) Ji, C.; Zheng, R.; Hou, D.; Zhu, H.; Wu, J.; Chyu, M. C.; Ma, Y. Pressure-Induced Phase Transition in Potassium Azide up to 55 GPa. *J. Appl. Phys.* **2012**, *111*, No. 112613.

(30) Hou, D.; Zhang, F.; Ji, C.; Hannon, T.; Zhu, H.; Wu, J.; Ma, Y. Series of Phase Transitions in Cesium Azide under High Pressure Studied by in Situ X-ray Diffraction. *Phys. Rev. B: Condens. Matter Mater. Phys.* **2011**, *84*, No. 064127.

(31) Zhang, M.; Yan, H.; Wei, Q.; Wang, H.; Wu, Z. Novel High-Pressure Phase with Pseudo-Benzene ″N6″ Molecule of LiN₃. *Europhys. Lett.* **2013**, *101*, No. 26004.

(32) Pringle, G. E.; Noakes, D. E. The Crystal Structures of Lithium, Sodium and Strontium Azides. *Acta Crystallogr., Sect. B: Struct. Crystallogr. Cryst. Chem.* **1968**, *24*, 262−269.

(33) Hendricks, S. B.; Pauling, L. The Crystal Structures of Sodium and Potassium Trinitrides and Potassium Cyanate and the Nature of the Trinitride Group. *J. Am. Chem. Soc.* **1925**, *47*, 2904−2920.

(34) Polak, M.; Gruebele, M.; Saykally, R. J. Velocity Modulation Laser Spectroscopy of Negative Ions. The ν₃ Band of Azide Anion. *J. Am. Chem. Soc.* **1987**, *109*, 2884−2887.

(35) Zintl, E.; Brauer, G. Konstitution des Lithiumnitrids. *Z. Elektrochem.* **1935**, *41*, 102−107.

(36) Barrett, C. S. X-ray Study of the Alkali Metals at Low Ttemperatures. *Acta Crystallogr.* **1956**, *9*, 671−677.

(37) Lonie, D. C.; Zurek, E. XtalOpt: An Open-Source Evolutionary Aalgorithm for Crystal Structure Prediction. *Comput. Phys. Commun.* **2011**, *182*, 372−387.

(38) Gray, P.; Waddington, T. C. Thermochemistry and Reactivity of the Azides. I. Thermochemistry of the Inorganic Azides. *Proc. R. Soc. London, Ser. A* **1956**, *235*, 106−119.

(39) The experimental study is not absolutely clear on whether DH°_f is positive or negative.

(40) Schneider, S. B.; Frankovsky, R.; Schnick, W. High-Pressure Synthesis and Characterization of the Alkali Diazenide Li₂N₂. *Angew. Chem., Int. Ed.* **2012**, *51*, 1873−1875.

(41) (a) Saxe, P.; Schaefer, H. F., III Cyclic *D*₆ₕ Hexaazabenzene—A Relative Minimum on the N₆ Potential Energy Hypersurface? *J. Am. Chem. Soc.* **1983**, *105*, 1760−1764. (b) Glukhovtsev, M. N.; Schleyer, P. v. R. Structures, Bonding and Energies of N₆ Isomers. *Chem. Phys. Lett.* **1992**, *198*, 547−554. (c) Fabian, J.; Lewars, E. Azabenzenes (Azines)—The Nitrogen Derivatives of Benzene with One to Six N Atoms: Stability, Homodesmotic Stabilization Energy, Electron Distribution, and Magnetic Ring Current; A Computational Study. *Can. J. Chem.* **2004**, *82*, 50−69. (d) Lewars, E. G. *Modeling Marvels*; Springer: New York, 2008; pp 151−155. (e) Gimarc, B. M.; Zhao, M. Strain Energies in Homoatomic Nitrogen Clusters N₄, N₆, and N₈. *Inorg. Chem.* **1996**, *35*, 3289−3297. (f) Nguyen, M. T.; Ha, T. K. Decomposition Mechanism of the Polynitrogen N₅ and N₆ Clusters and Their Ions. *Chem. Phys. Lett.* **2001**, *335*, 311−320. (g) Gagliardi, L.; Evangelisti, S.; Barone, V.; Roos, B. O. On the Dissociation of N₆ into 3 N₂ Molecules. *Chem. Phys. Lett.* **2000**, *320*, 518−522. (h) Wang, L. J.; Warburton, P.; Mezey, P. G. Theoretical Prediction on the Synthesis Reaction Pathway of N₆ (*C*₂ₕ). *J. Phys. Chem. A* **2002**, *106*, 2748−2752. (i) Li, Q. S.; Liu, Y. D. Theoretical Studies of the N₆ Potential Energy Surface. *J. Phys. Chem. A* **2002**, *106*, 9538−9542. (j) Hoffmann, R.; Hopf, H. Learning from Molecules in Distress. *Angew. Chem., Int. Ed.* **2008**, *47*, 4474−4481. (k) Hirshberg, B.; Gerber, R. B. Decomposition Mechanisms and Dynamics of N₆: Bond Orders and Partial Charges along Classical Trajectories. *Chem. Phys. Lett.* **2012**, *531*, 46−51.

(42) Li, Q. S.; Cheng, L. P. Aromaticity of Square Planar N₄²⁻ in the M₂N₄ (M = Li, Na, K, Rb, or Cs) Species. *J. Phys. Chem. A* **2003**, *107*, 2882−2889.

(43) (a) Burdett, J. K.; McLarnan, T. J. A Study of the Arsenic, Black Phosphorus, and Other structures Derived from Rock Salt by Bond-Breaking Processes. I. Structural Enumeration. *J. Chem. Phys.* **1981**, *75*, 5764−5773. (b) Burdett, J. K.; Haaland, P.; McLarnan, T. J. A Study of the Arsenic, Black Phosphorus, and Other Structures Derived From Rock Salt by Bondbreaking Processes. II. Band Structure Calculations and the Importance of the Gauche Effect. *J. Chem. Phys.* **1981**, *75*, 5774−5781. (c) Burdett, J. K.; Stephen, L. The Pressure-Induced Black Phosphorus to A7 (Arsenic) Phase Transformation: An Analysis Using the Concept of Orbital Symmetry Conservation. *J. Solid State Chem.* **1982**, *44*, 415−424.

(44) Zhu, W.; Xiao, J.; Xiao, H. Comparative First-Principles Study of Structural and Optical Properties of Alkali Metal Azides. *J. Phys. Chem. B* **2006**, *110*, 9856−9862.

(45) Babu, K. R.; Lingam, C. B.; Tewari, S. P.; Vaitheeswaran, G. High-Pressure Study of Lithium Azide from Density-Functional Calculations. *J. Phys. Chem. A* **2011**, *115*, 4521−4529.

(46) Dudarev, S. L.; Botton, G. A.; Savrasov, S. Y.; Humphreys, C. J.; Sutton, A. P. Electron-Energy-Loss Spectra and the Structural Stability of Nickel Oxide: An LSDA+U study. *Phys. Rev. B: Condens. Matter Mater. Phys.* **1998**, *57*, 1505−1509.

(47) The large *U*_eff seems unrealistic in comparison to the known charge-transfer metals where the proposed on-site Coulomb repulsion (*U*) is between 3 to 4 eV; see in the following: Garito, A. F.; Heeger, A. J. Design and Synthesis of Organic Metals. *Acc. Chem. Res.* **1974**, *7*, 232−240.

(48) (a) Ashcroft, N. W. Condensed-Matter Physics: Pressure for Change in Metals. *Nature* **2009**, *458*, 158−159. (b) Matsuoka, T.; Shimizu, K. Direct Observation of a Pressure-Induced Metal-to-Semiconductor Transition in Lithium. *Nature* **2009**, *458*, 186−189.

(c) Ma, Y.; Eremets, M.; Oganov, A. R.; Xie, Y.; Trojan, I.; Medvedev, S.; Lyakhov, A. O.; Valle, M.; Prakapenka, V. Transparent Dense Sodium. *Nature* **2009**, *458*, 182−185.

(49) Kresse, G.; Furthmüller, J. Efficient Iterative Schemes for *ab Initio* Total-Energy Calculations Using a Plane-Wave Basis Set. *Phys. Rev. B: Condens. Matter Mater. Phys.* **1996**, *54*, 11169−11186.

(50) Perdew, J. P.; Burke, K.; Ernzerhof, M. Generalized Gradient Approximation Made Simple. *Phys. Rev. Lett.* **1996**, *77*, 3865−3868.

(51) Blöchl, P. E. Projector Aaugmented-Wave Method. *Phys. Rev. B: Condens. Matter Mater. Phys.* **1994**, *50*, 17953−17979.

(52) Kresse, G.; Joubert, D. From Ultrasoft Pseudopotentials to the Projector Augmented-Wave Method. *Phys. Rev. B: Condens. Matter Mater. Phys.* **1999**, *59*, 1758−1775.

(53) Heyd, J.; Scuseria, G. E.; Ernzerhof, M. Hybrid Functionals Based on a Screened Coulomb Potential. *J. Chem. Phys.* **2003**, *118*, 8207−8215.

(54) Heyd, J.; Scuseria, G. E.; Ernzerhof, M. Erratum: Hybrid Functionals Based on a Screened Coulomb Potential [J. Chem. Phys. 2003, 118, 8207]. *J. Chem. Phys.* **2006**, *124*, 219906.

(55) Frisch, M. J.; Trucks, G. W.; Schlegel, H. B.; Scuseria, G. E.; Robb, M. A.; Cheeseman, J. R.; Scalmani, G.; Barone, V.; Mennucci, B.; Petersson, G. A.; Nakatsuji, H.; Caricato, M.; Li, X.; Hratchian, H. P.; Izmaylov, A. F.; Bloino, J.; Zheng, G.; Sonnenberg, J. L.; Hada, M.; Ehara, M.; Toyota, K.; Fukuda, R.; Hasegawa, J.; Ishida, M.; Nakajima, T.; Honda, Y.; Kitao, O.; Nakai, H.; Vreven, T.; Montgomery, J. A., Jr.; Peralta, J. E.; Ogliaro, F.; Bearpark, M.; Heyd, J. J.; Brothers, E.; Kudin, K. N.; Staroverov, V. N.; Kobayashi, R.; Normand, J.; Raghavachari, K.; Rendell, A.; Burant, J. C.; Iyengar, S. S.; Tomasi, J.; Cossi, M.; Rega, N.; Millam, J. M.; Klene, M.; Knox, J. E.; Cross, J. B.; Bakken, V.; Adamo, C.; Jaramillo, J.; Gomperts, R.; Stratmann, R. E.; Yazyev, O.; Austin, A. J.; Cammi, R.; Pomelli, C.; Ochterski, J. W.; Martin, R. L.; Morokuma, K.; Zakrzewski, V. G.; Voth, G. A.; Salvador, P.; Dannenberg, J. J.; Dapprich, S.; Daniels, A. D.; Farkas, Ö.; Foresman, J. B.; Ortiz, J. V.; Cioslowski, J.; Fox, D. J. *Gaussian 09*, Revision A.02; Gaussian: Wallingford, CT, 2009.

(56) Prasad, D. L. V. K.; Ashcroft, N. W.; Hoffmann, R. Lithium Amide ($LiNH_2$) Under Pressure. *J. Phys. Chem. A* **2012**, *116*, 10027−10036.

(57) Togo, A.; Oba, F.; Tanaka, I. First-Principles Calculations of the Ferroelastic Transition Between Rutile-Type and $CaCl_2$-type SiO_2 at High Pressures. *Phys. Rev. B: Condens. Matter Mater. Phys.* **2008**, *78*, No. 134106.

(58) Baroni, S.; Giannozzi, P.; Testa, A. Green's-Function Approach to Linear Response in Solids. *Phys. Rev. Lett.* **1987**, *58*, 1861−1864.

(59) Stokes, H. T.; Hatch, D. M.; Campbell, B. J. *ISOTROPY*, 2007, http://stokes.byu.edu/iso/findsym.html.

(60) Togo, A. http://spglib.sourceforge.net/

(61) Reflex Module in Materials Studio (6.1) of Accelrys, Inc.

(62) Momma, K.; Izumi, F. VESTA 3 for Three-Dimensional Visualization of Crystal, Volumetric and Morphology Data. *J. Appl. Crystallogr.* **2011**, *44*, 1272−1276.